

# Chapter 9

## LASER-INDUCED OCULAR EFFECTS IN THE RETINAL HAZARD REGION

DAVID J. LUND, BA,\* AND BRIAN J. LUND, PhD†

---

INTRODUCTION

BACKGROUND

WAVELENGTH DEPENDENCE

EXPOSURE DURATION

REPETITIVE PULSES

SUMMARY

\*Research Biophysicist (retired), US Army Medical Research Detachment, 7965 Dave Erwin Drive, Brooks City Base, Texas 78235

†Research Physicist, Ocular Trauma, US Army Institute of Surgical Research, 3698 Chambers Pass, Joint Base San Antonio, Fort Sam Houston, Texas 78234-7767

## INTRODUCTION

Researchers have actively investigated the interaction of laser radiation with retinal tissue *in vivo* for well over 40 years. A majority of the research has been funded by the Department of Defense primarily because of capability and need. Immediately after the first successful operation of a ruby laser, the US Army proceeded to adapt the device for use as a rangefinder. The laser presented an elegant solution to an old problem, but also presented a new, poorly understood problem. Military tacticians already fully understood and could fully exploit the consequences of directing a high-velocity projectile. The parameters of safe operation of traditional munitions were understood and drummed into new recruits in basic training. By contrast, the new laser could be fired repeatedly at an individual with no discernible effect, unless that individual was standing in the wrong place and looking in the wrong direction. In that case, the consequences of exposure could be devastating. The parameters of safe laser operation were not understood because the potential for harm had not yet been measured. Initial guidance was borrowed from studies that had been conducted in the 1950s and were designed to determine the retinal hazard of the nuclear fireball. But the laser was clearly different than other light sources; to resolve safety issues, it would be necessary to perform bioeffects experiments using the laser itself as a source. The military had the lasers, the applications, and the need to ensure the safety of its troops. Both the US Army and the US Air Force established multidisciplinary research teams in the late 1960s to initiate bioeffects experiments to determine the eye hazard posed by the lasers available at that time. Data developed by these teams provided a basis for the first standards for the safe use of lasers.

Since that time, researchers have continued to study the potential for damage of ever more sophisticated lasers using more sophisticated dosimetry and diagnostics. The total number of groups and individual investigators involved is small; the database of thresholds for laser-induced retinal damage is substantial, but by no means complete. A *primary purpose* of laser bioeffects research is to establish parameters for safe use and to serve as a basis for the establishment of safety guidelines. Laser safety guidelines are, in effect, an empirical model based on the trends of threshold data, which enables the computation of a maximum permissible exposure (MPE) for any given combination of laser parameters. The original guidelines were formulated around a rudimentary database and drew heavily on knowledge of the optical and physical characteristics of the eye, and from physical theories about how light interacts with matter in general and with biological tissue in particular.<sup>1-3</sup> The original guidelines have proven quite durable. Provisions of the guidelines have been adjusted and/or incremented to represent a growing body of supporting data, but many of the basic provisions for exposure time and wavelength dependence are essentially unaltered.

A *secondary purpose* of laser bioeffects research is to reach a point in which the database itself is sufficient. Based on existing data, it would seem useful to construct an empirical model that is capable of predicting the ED<sub>50</sub> (exposure dose having a 50% probability of producing the criterion response) for all exposure configurations. To the extent that such a model is successful, data are understood to be sufficient and self-consistent. Where the model is not successful, data are understood to be inadequate or contradictory. The model should, therefore, point to deficiencies in the available dataset and, by extension, to deficiencies in the provisions of the safety guidelines.

## BACKGROUND

The eye is the most vulnerable part of the body to visible and near-infrared (NIR) laser radiation. This is because the eye can concentrate incident light on the absorbing layers of retinal tissue that lie at the focus of the eye's optical system<sup>3-6</sup> (Figure 9-1). In the relaxed, normal eye, a collimated laser beam is focused into a small retinal image where the concentrated energy can induce thermal, mechanical, and photochemical processes that alter the retinal tissue.<sup>6-9</sup>

Researchers have accumulated a substantial body of dose-response data by introducing carefully controlled and measured energy into the eye of anesthetized animals, and evaluating the exposed retinas for resulting

alterations. A number of metrics have been used to determine the presence of alteration. The more sensitive metrics, such as measures of visual function and microscopic evaluation of excised tissue, are resource intensive; these metrics are utilized sparingly to place a lower bound on the range of introduced energy capable of producing retinal change. The primary metric continues to be the presence of a minimum visible lesion (MVL) detected via ophthalmic examination after exposure. Two methods have been used to estimate the introduced energy that is required to produce the MVL. Some researchers placed a graduated range of exposures on the retina and approximated threshold

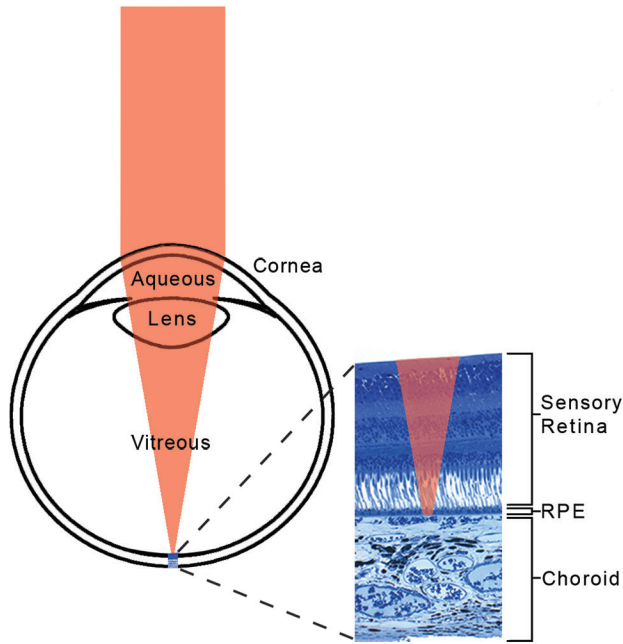


**Figure 9-1.** An incident laser beam is concentrated by the optics of the eye onto the retina. Light passes through the clear ocular media and the sensory retina before impinging on the retinal pigment epithelium (RPE) and the choroid. The retinal pigment epithelium is a monolayer of cells containing strongly absorbing melanin granules.

energy as the average of the lowest energy that produces the criterion effect, and the highest energy that does not produce the criterion effect. More commonly, researchers have placed an array of exposures over a range of introduced energies (Figure 9-2), correlated the response (presence or absence of an MVL) to the introduced energy for each exposure (Figure 9-3), and computed the probability of producing the criterion response as a function of introduced energy using the statistical technique of probit analysis.<sup>10,11</sup> The principal products of the probit analysis are the  $ED_{50}$  and the slope that can be given either as the slope,  $b$ , of the probit curve at the  $ED_{50}$  or as the ratio  $ED_{50}/ED_{84}$  where  $ED_{84}$  is that dose having an 84% probability of producing the criterion response. The two are related:  $b = [\log_{10}(ED_{50}/ED_{84})]^{-1}$ .

The  $ED_{50}$  is not a threshold; in fact, it may not be possible to determine a true threshold for these effects. The  $ED_{50}$  should, however, be related to the threshold in a manner that is persistent across exposure parameters and therefore serves as a fair and viable basis for safety guidelines. For the remainder of this chapter,  $ED_{50}$  will be the label for not only the product of a probit analysis, but also for the estimated dose for production of an MVL determined by other estimation techniques.



**Figure 9-2.** An array of laser exposures of varying incident energy in the retina of a rhesus monkey. The laser wavelength was 532 nm, and the exposure duration was 100 ms. Some exposures resulted in visible alteration while others did not.

The  $ED_{50}$  for laser-induced threshold damage is dependent on a number of factors. Inherent to the laser are wavelength, pulse duration, and pulse repetition rate. The experimental configuration determines the retinal irradiance area and profile, the exposure duration, and the number of pulses. The investigator

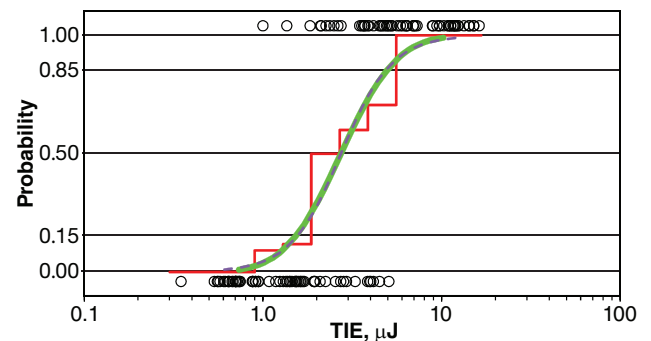


**Figure 9-3.** The probability of producing a minimum visible lesion (MVL) as a function of the incident energy. Exposures producing an MVL are placed on the probability = 1.0 axis. Exposures not producing an MVL are placed on the probability = 0 axis. The red line shows the probability of producing an MVL determined by dividing the number producing an MVL by the total number of doses in a range of incident energy. The green line is the probability of producing an MVL as determined by probit analysis of the data. The dashed line (on the green line) is the probability obtained by setting  $\alpha = ED_{50}$  (dose having a 50% probability of producing the criterion response) and  $B = b - 1$  in the logistic ogive (equation (9)).  $b$  is the slope of the probit fit. TIE: total intraocular energy

chooses the criterion for determination of retinal alteration. The scope of this chapter encompasses only the retinal MVL as determined by ophthalmic examination. The visibility of laser-induced retinal alteration varies with the interval between exposure and observation. Early researchers used 5- to 15-min observation times before standardizing on a 1-h endpoint. More recently, investigators have augmented the 1-h endpoint with a second observation at 24- to 48-h postexposure. The later observation typically results in a lower  $ED_{50}$ . Early researchers used the rabbit as the animal model, but later adopted the rhesus monkey as a closer match to the human eye. Within the primate

eye, the central area of the retina, known as the *macula*, is generally more sensitive to laser-induced alteration than are the more peripheral paramacular retinal areas. A single experiment, with exposures placed in both macular and paramacular retinal areas of the rhesus eye and with observation endpoints of 1 h and 24 h postexposure, can yield four distinct  $ED_{50}$  values, the lowest of which is the  $ED_{50}$  for macular alteration observed 24 h after exposure. The remainder of this chapter concerns the wavelength dependence of the  $ED_{50}$ , the exposure duration dependence of the  $ED_{50}$ , and the nature of the effects of repetitively pulsed retinal exposures.

### WAVELENGTH DEPENDENCE

Threshold-level laser-induced thermal retinal damage is localized to the retinal pigment epithelium (RPE), a monolayer of cells within the retina containing melanin granules (see Figure 9-1). Melanin is a very strong absorber of optical radiation to the extent that most of the radiation incident on the retina is absorbed in a 5  $\mu\text{m}$  layer of melanin granules. The absorbed energy results in significant tissue heating and thermal damage even for very low levels of energy incident at the cornea.

Assuming that the temperature required for threshold damage is not dependent on the wavelength of the incident radiation, an action spectrum for thermal retinal damage can be approximated based on the wavelength-dependent transmittance through the preretinal ocular media and absorption within the retina.<sup>1,6,12</sup> Transmittance of the preretinal ocular media has been measured by a number of investigators.<sup>13-19</sup>

The transmittance of the media, cornea, aqueous, lens, and vitreous was measured separately for each of the component parts after dissection of the eye. The tissue was necessarily “dead” with attendant changes in transmission and, more importantly, scatter of the transmitted light. Scattered light becomes very important for the determination of retinal irradiance in that it removes light from the focused beam, thus reducing the retinal irradiance. The primary source of scatter in the transmitted radiation is the cornea, and scatter in the cornea is sensitive to the integrity of its structure. Typically, the transmission of the tissue is measured in a spectrophotometer configured to collect all the transmitted radiation; thus, the measured quantity is the total transmission through the tissue. Transmission of the eye, based on these measurements, will overstate the irradiance at the retina. Alternately, the direct transmission of the ocular tissues is determined

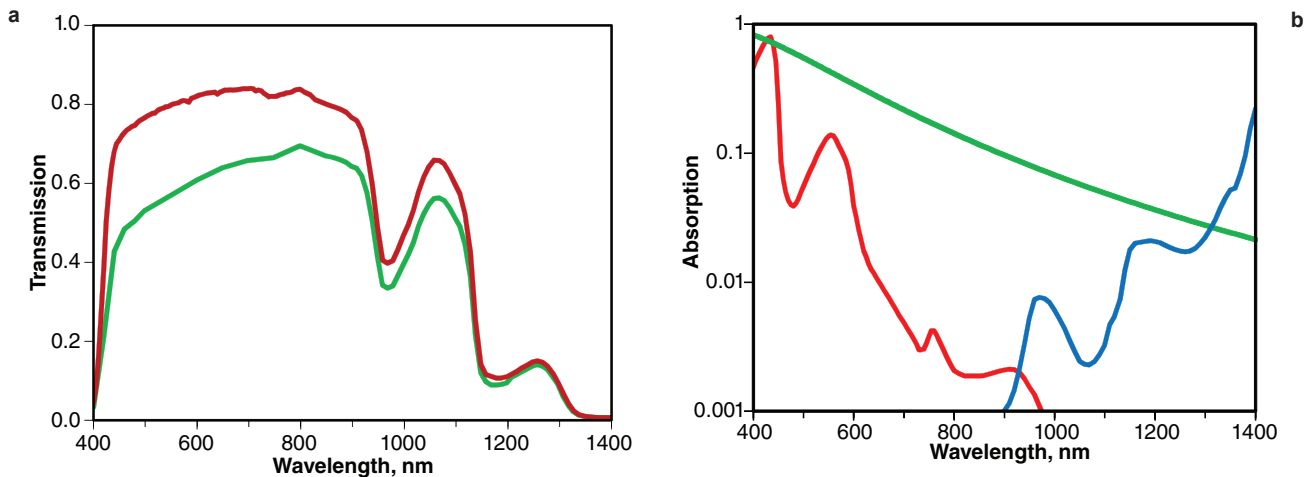


**Figure 9-4.** (a) Direct (green line) and total (red line) transmission ( $T_x$ ) of the preretinal ocular media of the rhesus eye. (b) Absorption ( $A_x$ ) of light in the retina by  $\text{H}_2\text{O}$  (blue line), oxyhemoglobin (red line), and retinal pigment epithelium (green line).

by collecting only the portion that remains collimated after traversing the tissue and thus will converge to a focus in the intact eye. Data from these studies have been collected and used as the basis for a consistent set of ocular transmittance tables published by the Commission Internationale de l'Éclairage (CIE).<sup>20</sup> The CIE tables of direct transmission of the rhesus eye are used in this chapter (Figure 9-4a). The choice of rhesus monkey is deliberate; essentially all available laser-induced retinal damage thresholds have been determined in that species, and the intent is to compare the theoretical action spectrum to the experimental data.

Energy reaching the retina is absorbed in the retina and choroid. The percentage of light absorbed in the RPE has been measured for the human, rabbit, and rhesus monkey. The values for RPE absorption used in this analysis (Figure 9-4b) are represented by the equation:

$$(1) \quad A(\lambda) = 1 - e^{-\alpha_\lambda s},$$

where  $s$  is the absorption length, and the absorption coefficient is given by  $\alpha_\lambda = \alpha_0(\lambda_0/\lambda)^{3.5}$ .

The absorption length,  $s$ , is  $5 \mu\text{m}$  and  $\alpha_0$  is set to  $4,100 \text{ cm}^{-1}$  at the wavelength  $\lambda_0$  of  $380 \text{ nm}$ . This form provided a reasonable fit to the experimentally determined absorption of the RPE.<sup>21-23</sup>

Before reaching the RPE in the macula and the region around the macula, light must traverse the neural retina that contains layers of capillaries having an average diameter of  $5 \mu\text{m}$ .<sup>24</sup> The absorption of incident radiation in  $5 \mu\text{m}$  of hemoglobin is equal to the absorption in

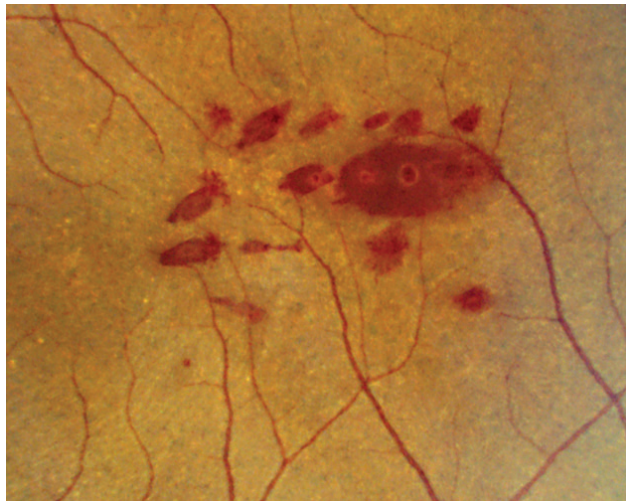


**Figure 9-5.** An array of laser exposures of varying incident energy in the retina of a rhesus monkey demonstrating a high incidence of retinal hemorrhage. The laser wavelength was  $430 \text{ nm}$ , and the exposure duration was  $3.5 \text{ ns}$ .

the RPE for the wavelength range around  $440 \text{ nm}$  (see Figure 9-4b). Figure 9-5 is representative of the retinal appearance after exposure to blue wavelength laser pulses of  $3.5\text{-ns}$  duration with the laser beam focused by the eye to  $\sim 25 \mu\text{m}$  diameter at the retina; this demonstrates the high incidence of retinal hemorrhage for such exposures. For exposure wavelengths from  $410$  to  $450 \text{ nm}$ , the hemorrhage resulted from rupture of capillaries in the neural retina, and the  $\text{ED}_{50}$  for the production of such hemorrhage was nearly the same as the  $\text{ED}_{50}$  for the production of RPE injury at the same wavelength (Figure 9-6). For wavelengths longer than  $450 \text{ nm}$ , the hemorrhage was subretinal, resulting from the rupture of Bruch's membrane at the RPE/choriocapillaris interface; the  $\text{ED}_{50}$  for such a hemorrhage was much higher than the  $\text{ED}_{50}$  for production of RPE injury.

At wavelengths longer than  $1,300 \text{ nm}$ , light absorption by  $\text{H}_2\text{O}$  in the sensory retina is as great as that absorbed in the RPE. The  $\text{H}_2\text{O}$ -absorbed energy can produce laser-induced thermal damage in all layers of the retina<sup>25</sup> (Figure 9-7).

The energy absorbed by the RPE,  $Q_r(\lambda)$ , is:

$$(2) \quad Q_r(\lambda) = Q_p(\lambda) \cdot T(\lambda) \cdot T_b(\lambda) \cdot A(\lambda),$$

where

$Q_p(\lambda)$  = the energy at the cornea within the area of the pupil,

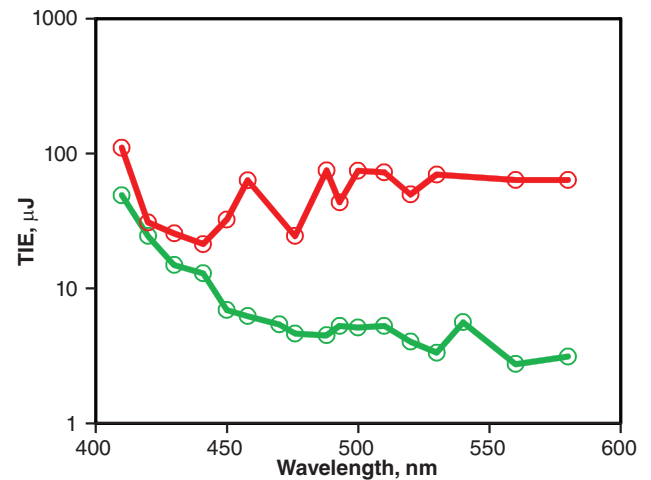


**Figure 9-6.** A comparison of the  $\text{ED}_{50}$  (dose having a 50% probability of producing the criterion response) for production of a minimum visible lesion (green line) in the retinal pigment epithelium to the  $\text{ED}_{50}$  for production of a retinal hemorrhage (red line) for laser retinal exposure in  $3.5\text{-ns}$  duration pulses to laser radiation at wavelengths from  $410$  to  $570 \text{ nm}$ .

TIE: total intraocular energy

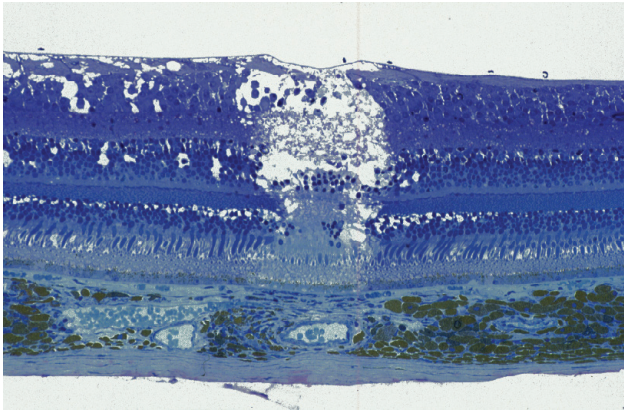


**Figure 9-7.** Laser-induced retinal injury in the rhesus monkey after exposure to a 20-ns duration pulse having a wavelength of 1,319 nm. High absorption of laser energy by the H<sub>2</sub>O in the retina resulted in damage in all retinal layers.

$T(\lambda)$  = the transmission of the preretinal ocular media at wavelength  $\lambda$ ,

$A(\lambda) = ARPE(\lambda) + AH20(\lambda)$  is the absorption of the retina at wavelength  $\lambda$ , and

$T_b(\lambda)$  = the transmission of hemoglobin (where a 5  $\mu\text{m}$  absorption path is assumed).

Rearranging,

$$(3) \quad Q_p(\lambda) = Q_r(\lambda) / \{T(\lambda) \cdot T_b(\lambda) \cdot A(\lambda)\}.$$

The absorbed energy,  $Q_{rx}$ , required to produce thermal tissue damage varies as a function of the diameter of the irradiated area on the retina. Given a collimated

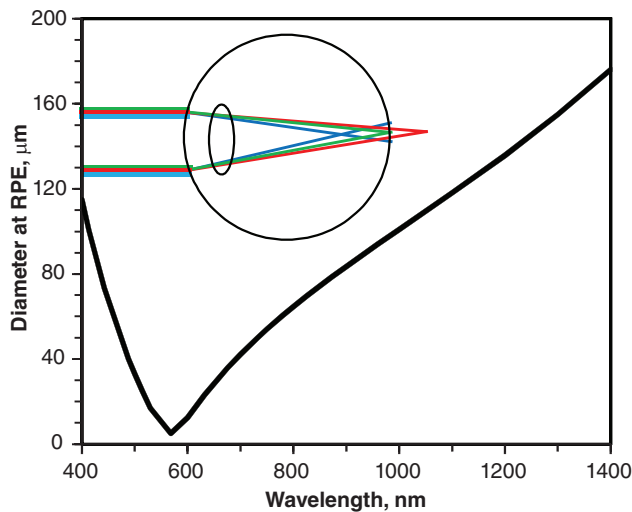


**Figure 9-8.** Chromatic-aberration-induced variation of the laser beam diameter at the retinal pigment epithelium (RPE) ( $d_\lambda$ ) of the rhesus eye for a collimated beam incident at the cornea. Blue, green, and red wavelengths are imaged at different retinal planes.

laser beam incident at the cornea, the diameter of the irradiated area at the RPE varies with the wavelength of the incident light because of chromatic aberration (Figure 9-8).<sup>26,27</sup>

The threshold for laser-induced retinal damage becomes larger as the irradiated area of the retina becomes larger (see Chapter 10, Dependence of Retinal Thermal Injury Threshold on Size and Profile of Laser). Therefore, a spot size-dependent term must be inserted into equation (3).

$$(4) \quad Qp(\lambda) = k \cdot (d\lambda)^X / (T(\lambda) \cdot T_b(\lambda) \cdot A(\lambda)),$$

where

$$k = Qr_0 / d_0^2$$

$Qr_0$  = the required energy for a minimum spot size,  $d_0$  and

$d_\lambda$  = the chromatic aberration-induced diameter at wavelength  $\lambda$ .

The value of the exponent  $X$  and therefore  $(d_\lambda)^X$  is time dependent.  $X$  varies from a value of 2 (nanosecond to microsecond-duration exposures) to a value of 1 (1-s duration and longer exposures). This relationship is complicated by uncertainty over the value of  $d_0$ . Although the optical quality of the eye will allow the incident laser radiation to be focused to a diameter at the RPE as small as 5 to 7  $\mu\text{m}$  under optimum conditions,<sup>28</sup> research suggests that the threshold for retinal injury does not decrease for image diameters  $<70 \mu\text{m}$ <sup>29-31</sup> (Figure 9-9).

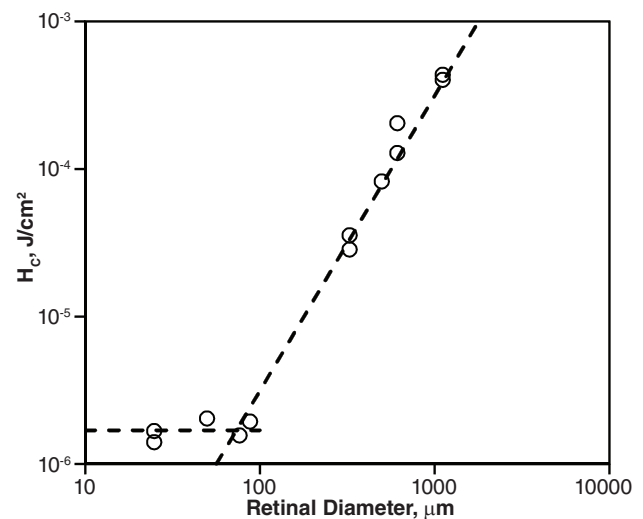


**Figure 9-9.** The dependence of ED<sub>50</sub> (dose having a 50% probability of producing retinal injury) on the retinal diameter ( $d$ ) for 7-ns duration, 532-nm laser exposures. Circles: measured values of the ED<sub>50</sub>. Dashed lines: trend lines fitted to the data.  $H_c$ : Radiant exposure measured at the cornea.

Experimental data relative to the wavelength dependence of the  $ED_{50}$  for retinal damage have been reported in the literature.<sup>12,32-39</sup> Data are shown in Figure 9-10. The corresponding  $Q_p(\lambda)$  curve was fit to each dataset by choosing the value of  $k$  to match the data at a single wavelength and choosing the value of  $X$  appropriate for the exposure duration. The value of  $d_0$  was set to 40  $\mu\text{m}$  except where the data were collected for larger retinal irradiance diameters. Over a broad range of exposure conditions, threshold laser-induced retinal damage can be fitted to curves derived from the assumption that the threshold injury is a thermal event driven by the laser energy absorbed in the RPE. Data shown include exposure durations from 3.5 ns to 16 s, wavelengths from 410 to 1,319 nm, and retinal irradiance diameters from the minimum the eye will produce to 350  $\mu\text{m}$ . Equation (4) produces a curve that matches the wavelength dependence of the data in all cases.

For most of the parameter space shown in Figure 9-10, laser-induced thermal injury is the dominant and limiting injury mechanism determining the laser hazard to the eye. When the wavelength is shorter than 550 nm and the exposure is longer than 10 s, laser irradiation can produce photochemical injury to the retina at doses significantly lower than those required to produce thermal injury.<sup>6,33,36</sup> These photochemical injury levels are omitted from Figure 9-10 for clarity.

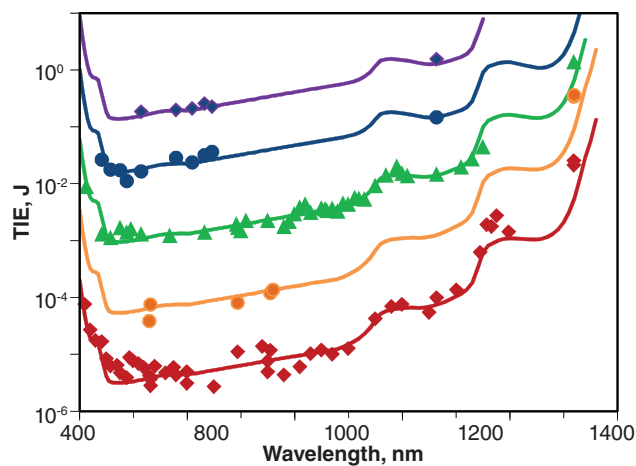


**Figure 9-10.** Wavelength dependence of  $ED_{50}$  (dose having a 50% probability of producing retinal injury) for laser-induced retinal alteration with  $Q_p$  matched to each dataset.  $t$  is the exposure duration, and  $d$  is the diameter of the irradiated retinal area. *Violet lines:*  $t = 16$  s,  $d = 350$   $\mu\text{m}$ ; *blue lines:*  $t = 1$  s,  $d = 350$   $\mu\text{m}$ ; *green lines:*  $t = 0.1$  s,  $d = 30$   $\mu\text{m}$ ; *orange lines:*  $t = 600$   $\mu\text{s}$ ,  $d = 30$   $\mu\text{m}$ ; and *red lines:*  $t = 3.5$  ns,  $d = 30$   $\mu\text{m}$ .

TIE: total intraocular energy

The ability to produce retinal lesions has been restricted to the wavelength range wherein the preretinal ocular transmission is  $\geq 1\%$ . Lesions have been produced in normal rhesus monkey eyes at 325 nm<sup>40</sup> and at 1,330 nm<sup>41,42</sup> near the short- and long-wavelength limits for retinal damage. Increasing the corneal dose to compensate for the preretinal loss does not extend the retinal damage range. Laser-induced alteration to the preretinal tissue limits the energy transmitted to the retina.

The eye is vulnerable to injury from laser radiation at wavelengths longer than 1,400 nm. The injury site is shifted to the cornea and lens, and the doses required to produce injury are higher because the incident radiation is no longer concentrated on the absorbing tissue by the optics of the eye. Although the database for laser-induced corneal injury is sparse compared to the data available for retinal thresholds, enough is available to match to a curve based on the 95% absorption depth of corneal tissue.<sup>42</sup> A continuation of injury level is seen through the transition from retinal injury to corneal injury at 1,400 nm, with a range at which both retinal and corneal injuries are possible (Figure 9-11).

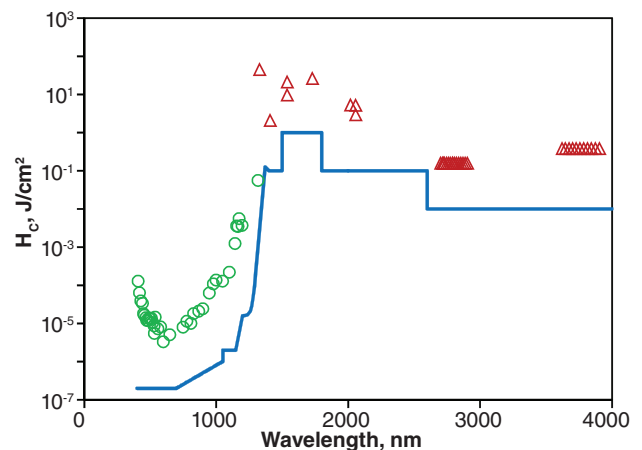


**Figure 9-11.**  $ED_{50}$  (dose having a 50% probability of producing retinal injury) for laser-induced ocular injury after exposure to nanosecond-duration laser irradiation. The thresholds are presented as corneal radiant exposure. When the injury site is the retina, the incident energy is averaged over a 7-mm diameter area at the cornea. The injury site is the retina for wavelengths shorter than 1,300 nm and the cornea for wavelengths longer than 1,400 nm. At 1,319 nm, both the cornea and the retina can be injured, but the threshold for retinal injury is lower. The American National Standards Institute's 2014 maximal permissible exposure for nanosecond-duration exposures is shown in ANSI Z136.1-2014 (American National Standard for the Safe Use of Lasers).

*Green circles:* measured retinal injury thresholds. *Red triangles:* measured corneal injury thresholds. *Blue line:* the 2014 maximum permissible exposure for ns-duration exposures.  $H_c$ : Radiant exposure measured at the cornea.

The MPE as provided in the 2007 and earlier editions of the laser safety standards was more than two orders of magnitude higher than the experimentally derived ED<sub>50</sub> at 1,330 nm. The safety factor was larger than necessary. Zuclich et al<sup>41</sup> proposed an adjustment of the wavelength dependence of the MPE for wavelengths between 1,250 and 1,400 nm to provide a better fit to the ED<sub>50</sub> data. In 2013, the International Commission

on Non-Ionizing Radiation Protection<sup>43</sup> (ICNIRP) accepted a modified version of that proposal that was then adopted in the 2014 editions of the American National Standards Institute (ANSI) Z136.1 (*Safe Use of Lasers*)<sup>44</sup> and the International Electrotechnical Commission (IEC) 60825-1 (*Safety of Laser Products*).<sup>45</sup> In Figure 9-12, data are compared to both the 2007 and the 2014 forms of the MPE.

### EXPOSURE DURATION

The ED<sub>50</sub> for in vivo laser-induced thermal retinal damage as a function of exposure duration is shown in Figure 9-13. For exposure durations of longer than a few microseconds, laser-induced retinal injury results from thermal coagulation of the retinal tissue; this is well explained by thermal models incorporating thermal conductivity of the tissue and the Arrhenius integral to signify damage due to denaturation of proteins.

A large body of data, supported by the thermal damage models, shows that for  $t$  greater than a few microseconds, the ED<sub>50</sub> varies as  $t^{3/4}$ , where  $t$  is the exposure duration. For exposures shorter than a few microseconds, the energy is deposited in times shorter than the thermal relaxation time of retinal tissue, leading to thermal confinement; thus, the energy required to produce a damaging temperature

rise is independent of the duration of the exposure. *Ex vivo* experiments designed to expose the RPE in retinal explants demonstrated that, for short-duration laser exposures, the threshold for laser-induced cell death correlates to the appearance of microcavitation (bubbles) around melanin granules superheated by incident laser irradiation.<sup>46-51</sup> Cell death almost always followed the induction of a bubble in the cell. Gerstman<sup>52</sup> showed theoretically that microcavitation occurred at lower incident irradiance than that required for Arrhenius thermal damage for pulses of duration between 1 ns and 1 μs. Experiments designed to distinguish between thermally induced damage and microcavitation-induced cell death showed that, for pulse durations of less than about 50 μs, the threshold-level damage mechanism transitions from thermal denaturation of proteins (as modeled by the Arrhenius integral) to a damage mechanism based on the formation of microcavitation bubbles around the melanosomes in the RPE. Figure 9-14 includes microcavitation-induced threshold values

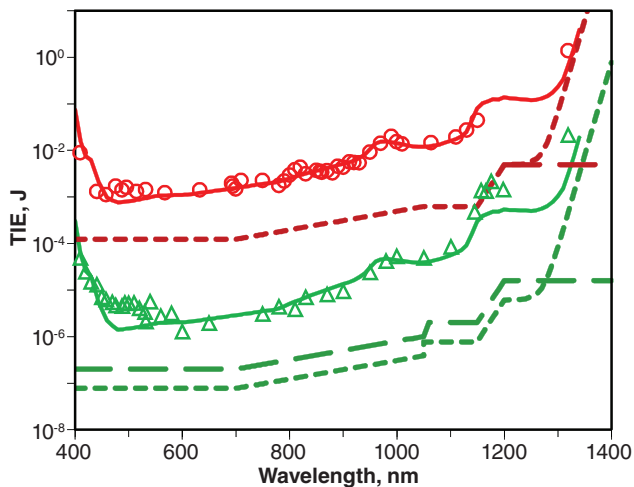


**Figure 9-12.** Wavelength-dependent ED<sub>50</sub> (dose having a 50% probability of producing the criterion response) data for nanosecond-duration laser exposures (green) and for 0.1-s duration laser exposures (red) in the rhesus eye.  $Q_{pv}$  has been fit to the data. The 2007 (long dashed lines) and the 2014 (short dashed lines) minimal permissible exposures are shown for each exposure duration. TIE: total intraocular energy

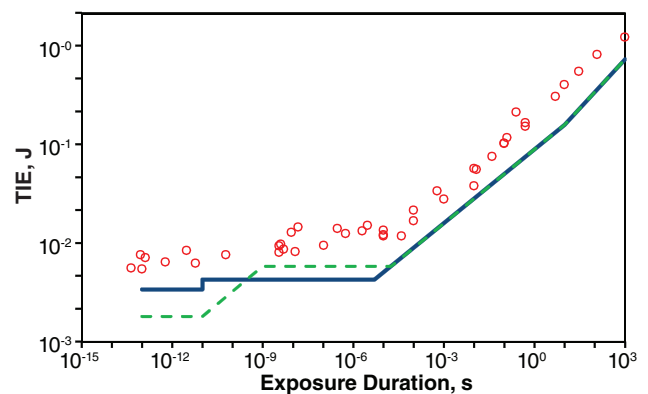


**Figure 9-13.** The time dependence of the ED<sub>50</sub> (dose having a 50% probability of producing retinal injury) for visible wavelength, laser-induced retinal damage. The 2007 (dashed line) and the 2014 (solid line) maximum permissible exposures for visible laser ocular exposure are included for comparison. Red circles: measured values of the ED<sub>50</sub>. TIE: total intraocular energy

for laser exposure in retinal explants from several studies.<sup>46,47,49,53-59</sup> The time dependence of these data is consistent with that of the in vivo data represented in Figure 9-13. Injury mechanisms for exposure durations shorter than 1 ns are discussed in Chapter 12, Ultrashort Laser Pulses and Their Bioeffects.

Recent experimentally determined laser-induced retinal injury threshold studies have been concentrated on determining the  $ED_{50}$  based on the detection of an MVL at 24-h postexposure for macular exposures in the rhesus monkey eye. For visible wavelength exposures of duration ranging from 3 to 100 ns, new data were within a factor of two to three times the MPE as provided by the 2007 standards.<sup>31,60-62</sup> The margin of safety was inadequate, considering the experimental uncertainties associated with the  $ED_{50}$  for short-pulse, collimated beam ocular exposure. In 2013, ICNIRP<sup>43</sup> accepted a recommendation to reduce the MPE for exposure durations below 5 ns by a factor of 2.5 to provide a larger safety margin that was then adopted in the 2014 editions of ANSI Z136.1<sup>44</sup> and IEC 60825-1<sup>45</sup>. The MPE, as provided by both the 2007 and 2014 guidelines, is included in Figure 9-13.

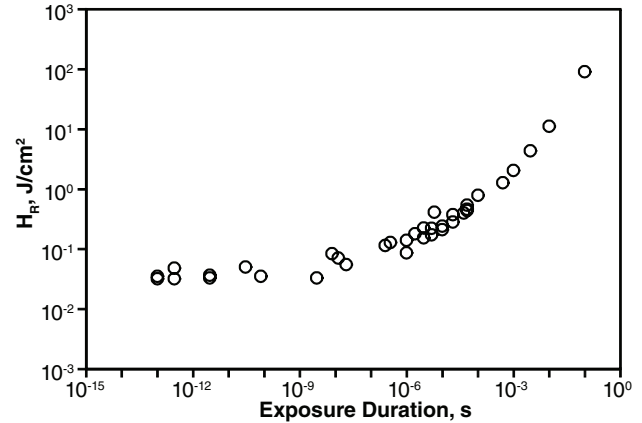


**Figure 9-14.** The  $ED_{50}$  (dose having a 50% probability of producing retinal injury) for thermally induced ex vivo (retinal explant) exposures. For pulse durations of less than about 50  $\mu$ s, the damage mechanism at threshold level changes from a thermal mechanism that can be well modeled by the Arrhenius integral to a damage mechanism based on the formation of microcavitation around the melanosomes in the retinal pigment epithelium. Circles: measured values of the  $ED_{50}$ .  $H_R$ : Radiant exposure at the retina.

## REPETITIVE PULSES

Laser safety guidelines provide three rules to be considered in the determination of the MPE for exposure to repetitive pulsed lasers. *Rule 1* simply states that no single pulse can exceed the MPE for exposure duration equal to the duration of the particular pulse. This is easily understood, because if a single pulse has enough energy itself to cause injury to the retina, it does not matter if any other pulses come before or after. *Rule 2* essentially says that if a number of pulses are delivered in an exposure time  $T$ , the average power in the pulsed beam shall not exceed the MPE for an exposure of duration  $T$ . This rule protects against injury due to accumulated photochemical damage mechanisms, as well as the buildup of heat in the retina. *Rule 3* states that the exposure for any single pulse in the train of pulses shall not exceed the single-pulse MPE multiplied by a multiple-pulse correction factor  $C_p$ . The purpose of Rule 3 is to protect against thermal injury caused by the buildup of heat from a series of subthreshold pulses.

The form of  $C_p$  has been rethought after the identification of microcavitation as a laser-induced retinal injury mechanism, and there is debate within the laser bioeffects research community as to whether or not Rule 3 can be eliminated entirely. In the 1983 edition of ANSI Z136.1, the multiple-pulse correction factor for Rule 3 was set to  $C_p = n^{-1/4}$ , where  $n$  is the number of pulses in the exposure.<sup>63</sup> The exposure limit for a multiple-pulse exposure is then given by

$$(5) \quad MPE(n.p.) = MPE(s.p.) \times n^{-1/4},$$

where  $MPE(n.p.)$  is the maximum permissible exposure for the repetitive-pulse train consisting of  $n$  pulses and is expressed as an energy per pulse.  $MPE(s.p.)$  is the maximum permissible exposure for a single pulse from the same laser. This form for the multiple-pulse correction factor was continued through the 2007 edition of ANSI Z136.1.

The  $n^{-1/4}$  relationship was first articulated by Stuck et al<sup>64</sup> based on an empirical fit to data reported in the literature. Laser-induced retinal injury threshold data for repetitive-pulse ocular exposures obtained from the literature<sup>42,64-68</sup> appear to confirm that the  $ED_{50}$ , expressed as energy per pulse, is well represented by a derating factor that varies as  $n^{-1/4}$  (Figure 9-15). This relationship can be expressed as:

$$(6) \quad ED_{50}(n.p.) = ED_{50}(s.p.) \times n^{-1/4}.$$

The relationship of equation (6) is independent of the wavelength, pulse duration, or pulse repetition frequency of the laser. Models based on a thermal damage mechanism cannot readily explain this result. Additivity of effect requires that each pulse must somehow sensitize the exposed retina, such that it becomes more susceptible to damage with each successive and cumulative pulse. Buildup of heat within the retina

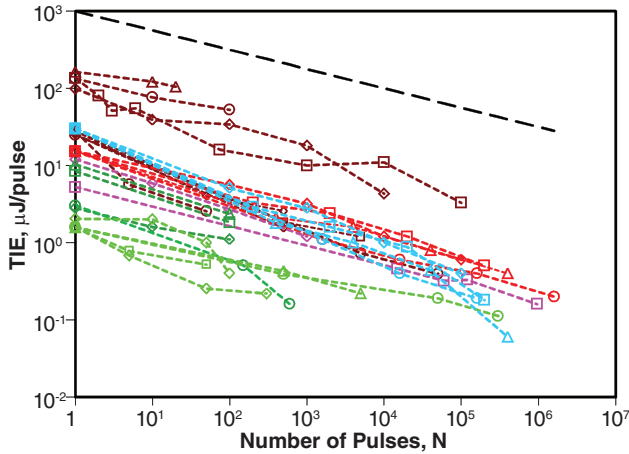


**Figure 9-15.** Laser-induced retinal injury threshold data for repetitive ocular exposures derived from the literature. The ED<sub>50</sub> (dose having a 50% probability of producing retinal injury), expressed as energy per pulse, is plotted as a function of the number of pulses, *n*. TIE: total intraocular energy

means that later pulses will require less energy to raise the temperature of the retina to the critical temperature that causes thermal damage. For a low pulse repetition frequency (or large interpulse spacing), diffusion of heat will allow the retina to cool, thus lessening the heat buildup. The fact that the  $n^{-1/4}$  dependence is independent of the interpulse spacing essentially rules out thermal memory as the mechanism.

Menendez et al<sup>69</sup> proposed a probability-summation model for predicting the threshold for a train of pulses based on the dose-response statistics for a single pulse. The model assumes that each pulse is an independent trial, that is, earlier pulses neither “sensitize” nor “harden” the retina to subsequent pulses. For the special case of a beam that consists of identical pulses (energy, pulse duration), the probability of a retinal response to each individual pulse can be assumed identically equal to *p*. In this case, the probability *P*(*n*) of inducing a retinal response after *n* pulses can be shown to be

$$(7) \quad P(n) = 1 - (1 - p)^n,$$

where *P*(*n*) = 0.5 for an ED<sub>50</sub>-level exposure. The response probability for each pulse of an ED<sub>50</sub>-level exposure to *n* pulses can then be determined by solving equation (7) for *p*:

$$(8) \quad p = 1 - (0.5)^{1/n}.$$

Menendez et al<sup>69</sup> assumed the single-pulse response probability was adequately described by the logistic ogive:

$$(9) \quad p = (1 + (D/\alpha)^{-\beta})^{-1},$$

where

*D* = the dose (pulse energy),

$\alpha$  = the ED<sub>50</sub> pulse energy for a single-pulse exposure, and

$\beta$  = related to the steepness of the dose-response curve.

Solving for *D* gives the pulse energy corresponding to the single-pulse response probability, *p*, obtained from equation (8):

$$(10) \quad D = \alpha(p^{-1} - 1)^{-1/\beta}.$$

As shown in Figure 9-3, when  $\alpha = ED_{50}$  and  $\beta = b - 1$ , where *b* is the slope of the probit curve, the logistic curve yields a relationship between dose and probability nearly identical to that predicted by the probit fit for 0.05 < *p* < 0.95.

Lund and Sliney<sup>70</sup> showed that, for a large number of pulses, the probability summation model led to the approximate relationship:

$$(11) \quad ED_{50}(n.p.) \sim ED_{50}(s.p.) \times n^{-1/(b-1)},$$

where *b* is the slope of the probit fit to the single-pulse, dose-response data. Equation (11) relates the ED<sub>50</sub>(*n.p.*), expressed as energy per pulse in a pulse train, to the ED<sub>50</sub>(*s.p.*) for a single pulse as a function of the number of pulses in the train and the slope (*b*) of the probit fit for a single-pulse exposure.

The mean value of the slope (*b*) of the probit fit is 4.8, as computed by the ProbitFit program<sup>11</sup> for more than 150 single-pulse threshold studies. Substituting *b* = 4.8 in equation (11) effectively reproduces equation (6). The probability summation model can explain the apparent success of the  $C_p = n^{-1/4}$  relationship. The unsettling thing about equation (11) is that ED<sub>50</sub>(*n.p.*) continues to decrease at the same rate as a function of *n* for an extremely large number of pulses, resulting in unreasonably small threshold values.

Equation (11) was derived with the aid of mathematical approximations, and assumed that the single-pulse dose-response data followed the logistic curve. However, the ED<sub>50</sub> values for laser-induced injury are typically inferred from exposure data using probit analysis, in which the dose-response curve is assumed to follow a log-normal distribution<sup>10,11</sup>:

$$(12) \quad p = \frac{1}{\sqrt{2\pi}} \int_{-\infty}^Y \exp\left(-\frac{t^2}{2}\right) dt.$$

In this equation, the probit value, *Y*, is given by:

$$(13) \quad Y = [x - \mu]/\sigma,$$

where

- $x = \log_{10}(\text{pulse energy});$
- $\mu = \log_{10}(\text{ED}_{50}(s.p.)),$  the base-ten logarithm of the ED<sub>50</sub> pulse energy for a single-pulse exposure; and
- $\sigma =$  the standard deviation of the log-normal distribution.

Equation (13) is a linear equation for  $Y$  as a function of  $x$ , and probit analysis involves finding the slope  $b$  and intercept  $a$  of the line  $Y = bx + a$  that best fits the dose-response data. The standard deviation of the single-pulse retinal response distribution is then given by  $\sigma = 1/b$ , and the  $\text{ED}_{50} = 10^{-a/b}$ .

Lund et al<sup>29,71</sup> examined multiple-pulse exposure data using probit analysis in conjunction with the probability summation model. For an  $n$ -pulse exposure, the per-pulse retinal response probability may be determined from equation (8). The probit value  $Y$  corresponding to this single-pulse response probability  $p$  is a function of the number of pulses  $n$  (equation (8)), and  $Y = Y(n)$  is also a function of  $n$ . The per-pulse energy at threshold,  $\text{ED}_{50}(n.p.)$  for an  $n$ -pulse exposure can then be calculated from the single-pulse  $\text{ED}_{50}$  by solving equation (13):

$$(14) \quad x = \mu + \sigma Y(n).$$

Inserting  $x = \log_{10}(\text{ED}_{50}(n.p.))$  and  $\mu = \log_{10}(\text{ED}_{50}(s.p.))$  gives

$$(15) \quad \text{ED}_{50}(n.p.) = \text{ED}_{50}(s.p.) \times 10^{\sigma Y(n)} = \text{ED}_{50}(s.p.) \times 10^{Y(n)/b}.$$

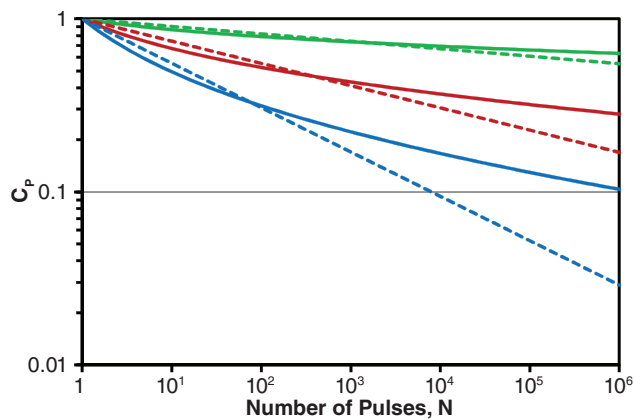


**Figure 9-16.** Comparison of the multiple-pulse correction factor ( $C_p$ ) for  $b = 24$  (typical of explant exposures; green lines),  $b = 8$  (typical of large spot *in vivo* exposures; red lines), and  $b = 5$  (typical of the data of figure 9; blue lines).  $b = 1/\sigma$  is the slope of the probit fit to the data. Dotted lines:  $C_p = n^{-1/(b-1)}$  (equation 11). Solid lines:  $C_p = 10^{Y(n)/b}$  (equation 15).

Equations (11) and (15) relate the  $\text{ED}_{50}(n.p.)$ , expressed as energy per pulse in a pulse train, to the  $\text{ED}_{50}(s.p.)$  for a single pulse as a function of the number of pulses in the train and the slope ( $b$ ) of the probit curve for a single-pulse exposure.

The values of  $b$  and therefore  $C_p = f(b)$  are in part a measure of experimental uncertainties in determining the single-pulse  $\text{ED}_{50}$ . Figure 9-16 compares the  $C_p$  as a function of  $n$  for a range of values of  $b$  for the exact solution and the approximate solution. Experimental uncertainties are reduced in threshold studies that use retinal explants as their model<sup>57,72</sup> and in the *in vivo* threshold studies wherein the diameter of the exposed retinal area is large.<sup>29,71</sup>

Figure 9-17 shows repetitive-pulse exposure threshold data obtained in retinal explant studies,<sup>46,54</sup> whereas Figure 9-18 shows repetitive pulse exposure threshold data obtained in large retinal irradiation diameter studies.<sup>29,71</sup> Data represented in these plots show that the experimentally determined value of  $C_p$  falls off much slower than  $n^{-1/4}$  when experimental uncertainties are reduced. A derating factor computed via equation (15) better matches the data and has the property that the  $\text{ED}_{50}(n.p.)$  decreases more slowly with increasing  $n$ .

It is not simple to translate equation (15) into a derating factor easily incorporated into the standards. Equation (11) is of the form already used to define the derating factor  $C_p$ . However, it requires a choice of the value of  $\beta$  (or  $b$ ). For the 1983 standard, the choice was effectively made to set  $\beta = 4$  based on available data. New data and analysis

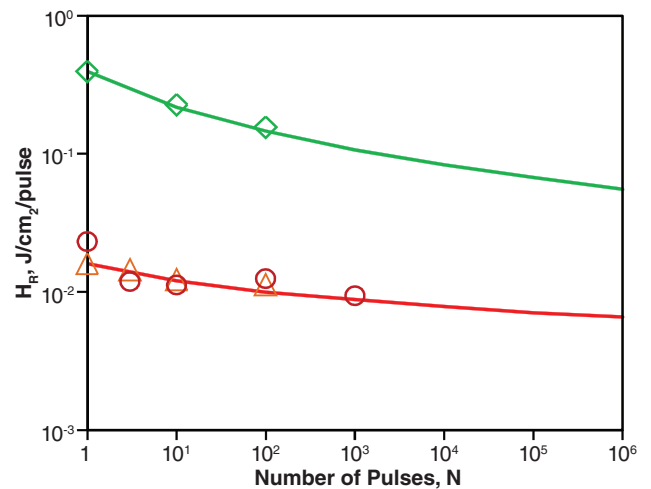


**Figure 9-17.** Repetitive-pulse exposure threshold data obtained in retinal explant studies by Brinkmann et al in 2000 (see reference 46) (green symbols) and by Roegenier et al in 2004 (see reference 54) (red symbols).  $H_R$ : Radiant exposure at the retina

suggest that this value is too low and results in overly conservative values of the MPE for large  $n$ . Lund and Sliney<sup>70</sup> and Sliney and Lund<sup>73</sup> argued that if indeed the value of the derating factor  $C_p$  was largely a function of experimental uncertainties, then the reduction afforded by this derating factor was already built into the MPE via the fact that the MPE was purposely set to a fraction of the  $ED_{50}$  to account for experimental uncertainties. Further reduction was therefore unnecessary, and  $C_p$  should be set to 1.0 for most exposure conditions. This suggestion motivated reevaluation of existing data and encouraged new studies. Given the required reduction of the single-pulse MPE for exposure durations shorter than a few microseconds, the value  $C_p = 1$  was found to provide a MPE level safe for essentially all of the credible available repetitive-pulse data.

Based on these considerations, the most recent guidelines for safe use of lasers<sup>44,45,74</sup> contain a revised formulation that sets the value of  $C_p = 1$  for most repetitive-pulse exposures.

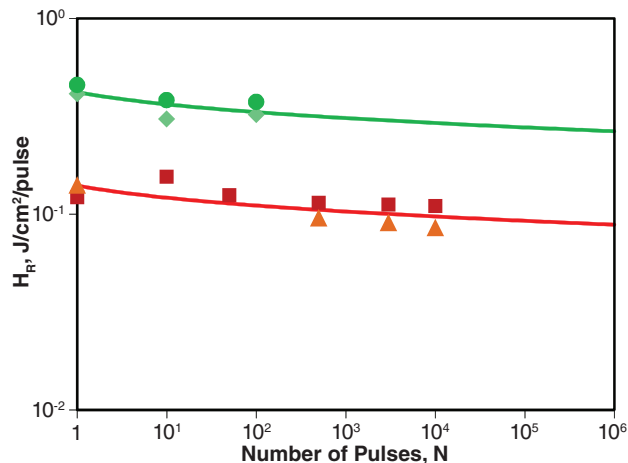


**Figure 9-18.** Repetitive-pulse exposure threshold data obtained *in vivo* for 7-ns duration, 532-nm laser exposure of retinal areas having diameters of 30 (green symbols), 100 (red squares), and 500  $\mu\text{m}$  (orange triangles) (see reference 29).  $H_R$ : Radiant exposure at the retina

## SUMMARY

The laser safety guidelines are, in effect, an empirical model that enables the computation of MPE for any given combination of laser parameters. Bioeffects research establishes the parameters for safe use of lasers and provides a basis for the establishment of guidelines. Although the bioeffects database is extensive and for the most part fully supports the safety guidelines, there are areas in which our understanding of specific damage mechanisms continues to evolve or in which the bioeffects data are not yet

accurately reflected in the safety guidelines. The threshold for laser-induced threshold damage is dependent on a number of factors. Inherent to the laser are its wavelength, pulse duration, and pulse repetition rate. The experimental configuration determines the retinal irradiance area and profile, the exposure duration, and the number of pulses. This chapter outlines our current understanding of how the threshold varies in each case with each of these parameters.

## REFERENCES

1. Borland RG, Smith PA, Owen GA. A model for the prediction of eye damage from pulsed lasers. *Lasers Light Ophthalmol.* 1992;5:61–67.
2. Sliney DH. The development of laser safety criteria: biological considerations. In: Wolbarsht ML, ed. *Laser Applications in Medicine and Biology*. New York, NY: Plenum Press; 1971: 163–238.
3. Sliney DH, Wolbarsht ML. *Safety With Lasers and Other Optical Sources*. New York, NY: Plenum Publishing Corp; 1980.
4. Beatrice ES, Randolph DI, Zwick H, Stuck BE, Lund DJ. Laser hazards: biomedical threshold investigations. *Mil Med.* 1977;14(11):889–892.
5. Ham WT Jr, Clarke AM, Geeraets WT, Cleary SF, Mueller HA, Williams RC. The eye problem in laser safety. *Arch Environ Health.* 1970;20:156–160.
6. Lund DJ. The new maximum permissible exposure: a biophysical basis. In: Barret K, ed. *Laser Safety: Tools and Training*. 2nd ed. Boca Raton, LA: CRC Press; 2014: 145–175.

7. Marshall J. Thermal and mechanical mechanisms in laser damage to the retina. *Invest Ophthalmol.* 1970;9:97–115.
8. Marshall J. Structural aspects of laser-induced damage and their functional implications. *Health Phys.* 1989;56(5):617–624.
9. Ham WT Jr, Ruffolo JJ, Mueller HA, Guerry D III. The nature of retinal radiation damage dependence on wavelength, power level, and exposure time. *Vision Res.* 1980;20:1105–1111.
10. Finney DJ. *Probit Analysis*. 3rd ed. New York, NY: Cambridge University Press; 1971.
11. Lund BJ. *The Probitfit Program to Analyze Data From Laser Damage Threshold Studies*. Brooks City-Base, TX: Walter Reed Army Institute of Research; 2006. WRAIR Report No. WTR/06-001, DTIC ADA452974.
12. Lund DJ, Edsall PR, Stuck BE. Spectral dependence of retinal thermal injury. *J Laser Applic.* 2008;20(2):76–82.
13. Geeraets WT, Berry ER. Ocular spectral characteristics as related to hazards from lasers and other light sources. *Am J Ophthalmol.* 1968;66:15–20.
14. Boettner EA, Dankovic D. *Ocular Absorption of Laser Radiation for Calculating Personnel Hazards: Determination of the Absorption Coefficient in the Rhesus Monkey*. Brooks Air Force Base, TX: US Air Force School of Aerospace Medicine; 1974. Final Report for Contract F41609-74-C-0008.
15. Boettner EA, Wolter JR. Transmission of the ocular media. *Invest Ophthalmol.* 1962;1:776–783.
16. Maher EJ. *Transmission and Absorption Coefficients for Ocular Media in the Rhesus Monkey*. San Antonio, TX: Brooks Air Force Base. AFB Report SAM-TR-78-32;1978.
17. Weisinger H, Schmidt FH, Williams DR, et al. The transmission of light through the ocular media of the rabbit eye. *Am J Ophthalmol.* 1956;42:907–910.
18. Ambach W, Blumthaler M, Schopf T, et al. Spectral transmission of the optical media of the human eye with respect to keratitis and cataract formation. *Doc Ophthalmol.* 1994;88:165–173.
19. Dillon J, Zheng L, Merriam J, Gaillard E. Transmission spectra of light to the mammalian retina. *Photochem Photobiol.* 2000;71:225–229.
20. Commission Internationale de l'Éclairage. *CIE 203-2012, A Computerized Approach to Transmission and Absorption Characteristics of the Human Eye*. Vienna, Austria: Commission Internationale de l'Éclairage; 2012.
21. Birngruber R, Hillenkamp F, Gabel VP. Theoretical investigations of laser thermal retinal injury. *Health Phys.* 1985;48(6):781–796.
22. Gabel VP, Birngruber R, Hillenkamp F. *Die Lichtabsorption am Augenhintergrund*. Munich, Germany: Gesellschaft für Strahlen- und Umweltforschung; 1976. GSF-Bericht A55.
23. Gabel VP, Birngruber R, Hillenkamp F. Visible and near infrared light absorption in pigment epithelium and choroid. In: *International Congress Series No. 450: XXIII Concillium Ophthalmologicum Kyoto*. Amsterdam, The Netherlands: Oxford-Excerpta Medica; 1978.
24. Lund DJ, Edsall PR, Stuck BE. Ocular hazards of Q-switched blue wavelength lasers. *Proc SPIE.* 2001;4246:44–53.
25. Lund DJ, Edsall PR, Stuck BE. Ocular hazards of Q-switched near-infrared lasers. *Proc SPIE.* 2003;4943:85–90.
26. Vincelette RL, Welch AJ, Thomas RJ, Rockwell BA, Lund DJ. Thermal lensing in ocular media exposed to continuous wave, near-infrared radiation: the 1150–1350 nm region. *J Biomed Optics.* 2008;13(5):054005.
27. Thomas RJ, Vincelette RL, Clark CD, Stolarski J, Irvin LJ, Buffington GD. Propagation effects in the assessment of laser damage thresholds in eye and skin. *Proc SPIE.* 2007;6435:64350A.

28. Birngruber R, Dreschel E, Hillankamp F, Gabel VP. Minimum spot size on the retina formed by the optical system of the eye. *Int Ophthalmol*. 1979;1(3):175–178.
29. Lund BJ, Lund DJ, Edsall PR. Damage threshold from large retinal spot size repetitive-pulse laser exposures. *Health Phys*. 2014;107(4):292–299.
30. Lund DJ, Edsall PR, Stuck BE, Schulmeister K. Variation of laser-induced retinal injury with retinal irradiated area: 0.1 s, 514 nm exposures. *J Biomed Opt*. 2007;12(2):06180.
31. Zuclich JA, Edsall PR, Lund DJ, et al. New data on the variation of laser-induced retinal damage threshold with retinal image size. *J Laser Applic*. 2008;20(2):83–88.
32. Connolly JS, Zuclich JA, Nawrocki DA, et al. *Research on the Effects of Laser Radiation*. Brooks Air Force Base, TX: Technology Incorporated; 1975. US Air Force School of Aerospace Medicine Contract F41609-73-C-0016. Second Annual Report.
33. Ham WT Jr, Mueller HA, Ruffolo JJ, Clarke AM. Sensitivity of the retina to radiation damage as a function of wavelength. *Photochem Photobiol*. 1979;29:735–743.
34. Ham WT Jr, Mueller HA, Sliney DH. Retinal sensitivity to damage from short wavelength light. *Nature*. 1976;260:153–155.
35. Lund DJ, Beatrice ES. Near infrared laser ocular bioeffects. *Health Phys*. 1989;56(5):631–636.
36. Lund DJ, Stuck BE, Edsall PR. Retinal injury thresholds for blue wavelength lasers. *Health Phys*. 2006;90(5):477–484.
37. Onda Y, Kameda T. *Studies of Laser Hazards and Safety Standards. Part 2. Retinal Damage Thresholds for Helium-Neon Lasers*. Fort Detrick, MD: Technological Research and Development Institute, Japan Defense Agency, and US Army Medical Intelligence and Information Agency; 1979. Translation no. USAMIIA-K9991.
38. Onda Y, Kameda T. *Studies of Laser Hazards and Safety Standards. Part 3. Retinal Damage Thresholds for Argon Lasers*. Fort Detrick MD: Technological Research and Development Institute, Japan Defense Agency, and US Army Medical Intelligence and Information Agency; 1979. Translation no. USAMIIA-K9992.
39. Zuclich JA, Griess GA, Harrison JM, Brakefield JC. *Research on the Ocular Effects of Laser Radiation*. Brooks Air Force Base, TX: US Air Force School of Aerospace Medicine; 1979. Report SAM-TR-79-4.
40. Zuclich JA, Connolly JS. Ocular damage induced by near-ultraviolet laser radiation. *Invest Ophthalmol*. 1976;15(9):760–764.
41. Zuclich JA, Lund DJ, Stuck BE. Wavelength dependence of ocular damage thresholds in the near-IR to far-IR transition region: proposed revisions to MPEs. *Health Phys*. 2007;92(1):15–23.
42. Lund DJ, Stuck BE, Beatrice ES. *Biological Research in Support of Project MILES*. Presidio of San Francisco, CA: Letterman Army Institute of Research Institute; 1981. Report 96.
43. International Commission on Non-Ionizing Radiation Protection. Revision of guidelines on limits of exposure to laser radiation of wavelengths between 400 nm and 1.4 mm. *Health Phys*. 2000;29(4):431–440.
44. American National Standards Institute. *ANSI Z136.1-2014: American National Standard for the Safe Use of Lasers*. Orlando, FL: Laser Institute of America; 2014.
45. International Electrotechnical Commission. *IEC 60825-1: Safety of Laser Products. Part 1. Equipment Classification, Requirements and Users Guide*. 3.0 ed. Geneva, Switzerland: IEC; 2014.
46. Brinkmann R, Hüttmann G, Roegerer J, Roeder J, Birngruber R, Lin CP. Origin of retinal pigment epithelial cell damage by pulsed laser irradiance in the nanosecond to microsecond time regimen. *Lasers Surg Med*. 2000;27:451–464.

47. Kelly MW. *Intracellular Cavitation as a Mechanism of Short-Pulse Laser Injury to the Retinal Pigment Epithelium* [PhD thesis]. Medford, MA: Tufts University; 1997.
48. Kelly MW, Lin CP. Microcavitation and cell injury in RPE cells following short-pulsed laser irradiation. *Proc SPIE*. 1997;2975:174–179.
49. Lin CP, Kelly MW, Sibayan SAB, Latina MA, Anderson RR. Selective cell killings by microparticle absorption of pulsed laser radiation. *IEEE J Sel Top Quantum Electron*. 1999;5(4):963–968.
50. Roegerer J, Lin CP. Photomechanical effects—experimental studies of pigment granule absorption, cavitation and cell damage. *Proc SPIE*. 2000;3902:35–40.
51. Roeder J, El Hifnawi E, Birngruber R. Bubble formation as primary interaction mechanism in retinal exposure with 200 ns laser pulses. *Lasers Surg Med*. 1998;27(5):451–464.
52. Gerstman B. Theoretical modeling of laser-induced explosive pressure generation and vaporization in pigment cells. *Proc SPIE*. 2000;3902:41–53.
53. Payne DJ, Thomas R, Elliot JJ, et al. Cavitation thresholds in the rabbit retina pigmented epithelium. *Proc SPIE*. 1999;3601:27–31.
54. Roegerer J, Brinkmann R, Lin CP. Pump-probe detection of laser induced microbubble formation in retinal pigment epithelium cells. *J Biomed Opt*. 2004;9(2):367–371.
55. Lee H, Alt C, Pitsillides CM, Lin CP. Optical detection of intracellular cavitation during selective laser targeting of the retinal pigment epithelium: dependence of cell death mechanism on pulse duration. *J Biomed Opt*. 2007;12(6):064034.
56. Schüle G, Rumohr M, Hüttmann G, Brinkman R. RPE damage thresholds and mechanisms for laser exposure in the microsecond-to-millisecond time regimen. *Invest Ophthalmol Vis Sci*. 2005;46(2):714–719.
57. Schulmeister K, Husinski J, Seiser B, et al. Ex vivo and computer model study on retinal thermal laser-induced damage in the visible wavelength range. *J Biomed Opt*. 2008;13(5):054038.
58. Neumann J, Brinkmann R. Cell disintegration by laser-induced transient microbubbles and its simultaneous monitoring by interferometry. *J Biomed Opt*. 2006;11(4):041112.
59. Alt C, Pitsillides V, Roegner J, Lin C. Monitoring intracellular cavitation during selective targeting of the pigment epithelium. *Proc SPIE*. 2003;4951:48–55.
60. Lund BJ, Lund DJ, Edsall PR. Laser-induced retinal damage threshold measurements with wavefront correction. *J Biomed Opt*. 2008;13(6):064011.
61. Lund BJ, Lund DJ, Holmes ML. Retinal damage thresholds in the 1 ns to 100 ns exposure duration range. In: *Proceedings of the International Laser Safety Conference, San Jose, California, 14–17 March 2011*. Orlando, FL: Laser Institute of America; 2011: 183–186.
62. Cain CP, Toth CA, DiCarlo CD, et al. Visible retinal lesions from ultrashort laser pulses in the primate eye. *Invest Ophthalmol Vis Sci*. 1995;36(5):879–888.
63. American National Standards Institute. *ANSI Z136.1-1983: American National Standard for the Safe Use of Lasers*. Cincinnati, OH: Laser Institute of America; 1983.
64. Stuck BE, Lund DJ, Beatrice ES. *Repetitive Pulse Laser Data and Permissible Exposure Limits*. San Francisco, CA: Letterman Institute of Research; 1978. Report 58.
65. Griess GA, Blankenstein MF, Williford GG. Ocular damage from multiple-pulse laser exposure. *Health Phys*. 1980;39:921–927.

66. Zuclich JA, Blankenstein MF. *Additivity of Retinal Damage for Multiple Pulse Laser Exposures*. Brooks Air Force Base, TX: US Air Force School of Aerospace Medicine; 1988. Report TR-88-24.
67. Ham WT Jr, Mueller HA, Wolbarsht ML, Sliney DH. Evaluation of retinal exposures from repetitively pulsed and scanning lasers. *Health Phys.* 1988;54(3):337–344.
68. Cain CP, Noojin GD, Stolarski DJ, Rockwell BA. Visible lesion thresholds from multiple pulse near infrared ultrashort laser pulses in the retina. *Health Phys.* 2002;86(6):855–862.
69. Menendez AR, Cheney FE, Zuclich JA, Crump P. Probability-summation model of multiple laser-exposure effects. *Health Phys.* 1993;65(5):523–528.
70. Lund DJ, Sliney D. A new understanding of multiple-pulsed laser-induced retinal injury thresholds. *Health Phys.* 2014;106(4):505–515.
71. Lund BJ, Lund DJ, Edsall PR, Gaines VD. Laser-induced retinal damage threshold for repetitive-pulse exposure to 100-ms pulses. *J Biomed Opt.* 2014;19(10):105006.
72. Lund DJ, Lund BJ. The determination of laser-induced injury thresholds. In: *Proceedings of the International Laser Safety Conference, Albuquerque, New Mexico, 23–26 March 2015*. Orlando, FL: Laser Institute of America; 2015: 69–73.
73. Sliney DH, Lund DJ. Do we overstate the risk of multiple pulsed exposure? In: *Proceedings of the International Laser Safety Conference, Reno, Nevada, 23–26 March 2009*. Orlando, FL: Laser Institute of America; 2009: 93–97.
74. International Commission on Non-Ionizing Radiation Protection. Guidelines on limits of exposure to laser radiation of wavelengths between 180 nm and 1000 nm. *Health Phys.* 2013;105(3):271–295.